



# A feasibility study on green biorefinery of high lignin content agro-food industry waste through supercritical water treatment

Tijana Adamovic<sup>a</sup>, Dmitry Tarasov<sup>b</sup>, Emre Demirkaya<sup>a</sup>, Mikhail Balakshin<sup>b</sup>,  
Maria José Cocero<sup>a,\*</sup>

<sup>a</sup> BioEcoUva, Research Institute, High Pressure Process Group, Department of Chemical Engineering and Environmental Technology, Valladolid University, Doctor Mergelina S/n, 47011, Valladolid, Spain

<sup>b</sup> Department of Bioproducts and Biosystems, School of Chemical Engineering, Aalto University, P.O. Box 16300, 00076, Aalto, Finland

## ARTICLE INFO

Handling editor: Prof. Jiri Jaromir Klemes

### Keywords:

Grape seeds  
Carbohydrates  
Polyaromatics  
Lignin  
2D-NMR analysis  
Circular economy

## ABSTRACT

This work discusses hydrolysis of defatted grape in supercritical water (SCW) at 380 °C and 260 bar from 0.18 s to 1 s focusing attention to sugars recovery in the liquid phase of the product and detailed characterization of remaining solid phase enriched in polyaromatics (e.g. lignin, flavonoids, etc.). After the longest reaction time of 1 s, 56% of carbohydrates could be recovered in the liquid phase, as a result of carbohydrate hydrolysis. The high content of insoluble lignin in biomass (36%), acts as a mass transfer limitation and presents an important feature in the hydrolysis process, slowing down the conversion of carbohydrate fraction, as after the maximum time of 1s, 10% of carbohydrates still remained in the solid phase. Milled wood lignin, extracted from biomass and dioxane extract from the solid phase were characterized in order to understand the main structural changes during the SCW hydrolysis process. Dioxane (80%) extraction of solids produces a very complex mixture of lipophilic extractives, flavonoids and lignin with a certain amount of chemically linked carbohydrates. 2D NMR analysis of dioxane extract shows remarkably subtle changes in the amounts of main lignin moieties ( $\beta$ -O-4',  $\beta$ - $\beta'$  (resinol) and  $\beta$ -5 (phenylcoumaran)). This subtle change of the main lignin structures is an important feature in the further valorisation of this sulfur-free lignin residue.

## 1. Introduction

Sugars or/and bioethanol are the main objective of the current biorefinery. This approach does not pay enough attention to other valuable biomass compounds including lignin and further polyphenols that are an alternative sustainable source of high value chemicals (Balakshin et al., 2021). Biorefinery that targets just biofuel loses the utility of remaining compounds and struggle with significant economic challenges that are preventing further industrial development. This can be overcome by the implementation of the advanced integrated biorefinery approach that puts forward valorisation of every biomass stream for high value products (Balakshin et al., 2021).

One of the main challenges on the way of lignocellulosic biomass fractionation is its recalcitrance (Cocero et al., 2018). Biomass recalcitrance arises from three main constituents, cellulose, hemicellulose and lignin, and interaction between them (Lorenci Woiciechowski et al., 2020). Those three biopolymers create very compact, stable and resistant cell wall, so that significant force is required to separate them

(Lorenci Woiciechowski et al., 2020). Conventional methods used to fractionate biomass described well in literature are acid and enzymatic hydrolysis. Prior to enzymatic hydrolysis of biomass pre-treatment steps are needed in order to remove recalcitrance barriers and increase enzymatic digestibility (Hendriks and Zeeman, 2009). Pre-treatment includes physical, chemical, physicochemical or biological methods, or their combination (Lukajtis et al., 2018). The pre-treatment step is considered as the crucial step to enhance enzymatic efficiency but it is the most costly step of the process (Capolupo and Faraco, 2016), where also degradation reaction of targeted carbohydrates fractions occurs (Jung and Kim, 2015). Due to the enzymes prices the enzymatic hydrolysis itself is an expensive step (Capolupo and Faraco, 2016). Concentrated acid hydrolysis uses high acid concentration (over 30%) at ambient and moderated temperatures (<100 °C) to obtain high sugar yield without additional enzymatic hydrolysis step (Jung and Kim, 2015). No need for additional enzymatic hydrolysis step is one of the main advantages of this process while as the main disadvantage is considered the highly corrosive nature of used acids, that require

\* Corresponding author.

E-mail address: [mjcocero@iq.uva.es](mailto:mjcocero@iq.uva.es) (M.J. Cocero).

<https://doi.org/10.1016/j.jclepro.2021.129110>

Received 27 March 2021; Received in revised form 7 September 2021; Accepted 18 September 2021

Available online 27 September 2021

0959-6526/© 2021 The Authors.

Published by Elsevier Ltd.

This is an open access article under the CC BY-NC-ND license

(<http://creativecommons.org/licenses/by-nc-nd/4.0/>).

expensive equipment and steps of acid recovery due to the economic and environmental concerns (Solarte-Toro et al., 2019). As an alternative to conventional methods, we discuss the use of Supercritical water technology as a clean and powerful method for fractionation and valorisation of biomass to produce biorefinery lignin and to recover the carbohydrate fractions.

Attraction to use water as reaction medium commence due to its environmentally friendly and non-expensive advantages over other solvents. At supercritical conditions, water changes its character from a solvent for ionic species as it is at ambient conditions, to a solvent for non-ionic species, in which many biomass compounds have enhanced solubility. The dipole moment decreases to a value typical for organic solvents. The value of pH significantly decreases in the subcritical region compared to ambient conditions, supplying in this way much more  $H_3O^+$  ions for acid catalysed reactions. The ionic product changes remarkably close to the critical temperature, turning near-critical and supercritical water into a much less ionized compound compared to water at ambient conditions (Brunner, 2014). The opportunity to affect the water properties by changing the pressure and temperature, shifting from polar to non-polar solvent and from ionic to radical favourable medium, allows to control selectivity in the process. The transport properties of supercritical water can successfully face biomass rigidity and complexity, as its low viscosity and high diffusivity facilitate penetration into biomass structure (Cocero et al., 2018). SCW environment provides an opportunity to conduct reactions in a single fluid phase, taking the advantages of having no interphase mass transport processes to decrease the reaction rate (Cantero et al., 2015a). As a result, reactions occur significantly faster. The reduction of reaction time allows a feasible scale up of the process, using small reaction volumes.

Grape seeds are the main by-product from grape processing, such as wine and grape juice industry. Above 3 Mt of grape seeds are discarded annually on the world base (Aristizábal-Marulanda et al., 2017). In the last few decades there has been rising interest in the valorisation of those products, to recover oil and phenolic compounds (Bravi et al., 2007; Duba et al., 2015; Fiori et al., 2014; Marqués et al., 2013). Oil from grape seeds is rich in unsaturated fatty acids such as linoleic acid and has furthermore a high content of tannins, that makes it more resistant to peroxidation (Cao and Ito, 2003). Grape seeds have been also appreciated because of their content of phenolic compounds and their extracts have been a subject of intensive investigation due to their potential beneficial effects on human health, such as antioxidant activity (Maier et al., 2009). After the extraction of oil, defatted seeds are considered as a residue and can be used to produce energy by combustion. Considering that this residue still contains significant amounts of carbohydrates and high amounts of polyaromatics (lignin and other polyphenols), further exploitation to recover and use remaining fractions could be more effective than energy recovery.

Previous work in our group has proved the practicability of sugar production from wheat bran and sugar beet pulp, in a continuous ultrafast supercritical hydrolysis pilot plant by the so-called FASTSUGAR process, demonstrating the challenges but also versatility and potential of the process (Martínez et al., 2019). This work is performed to discuss the feasibility of the SCW hydrolysis process for fractionation of biomass with high lignin content, as the amount of acid-insoluble lignin contained in defatted grape seeds is significantly higher compared to the amount in previously used biomass (36% is defatted grape seeds compared to 4% in sugar beet pulp and 2% in wheat bran) (Martínez et al., 2019). High lignin content biomass presents even greater challenge for the biorefinery, as lignin acts as a physical barrier that protects biomass from microorganism attack and chemical degradation, contributing significantly to biomass recalcitrance (Li et al., 2016; Loow et al., 2016). Characterization of lignin contained in defatted grape seeds is presented, as characterization of this lignin, to our knowledge, has not been reported before. Attention is focused on understanding the structural changes of lignin due to the supercritical water hydrolysis (SCWH) process, using among others 2D NMR as a powerful tool in

lignin analysis. Structural changes occurring on the lignin structure after SCW hydrolysis of biomass were also reported by Moon et al. but using woody biomass and more severe hydrolysis conditions in the terms of time (Moon et al., 2011). Characterization of lignin residue after supercritical water and understanding of structural changes caused in lignin structure are the first steps on the way of targeting possible application of this lignin residue.

Application of green technologies as SCW hydrolysis to valorise defatted grape seeds, help us to take further steps towards new environmentally compatible and sustainable chemicals and materials. In the further text we discuss our perspective on how valorisation of defatted grape seeds using supercritical water technology fits the 12 principles of green engineering (Anastas and Zimmerman, 2007):

**Inherent rather than circumstantial.** Defatted grape seeds are a by-product of grape seed oil production. The SCWH process requires thermal and electrical energy. The use of a gas turbine can lead to zero-energy consumption in the process, where the detailed explanation of heat integration with calculations can be found in the previous work (Cantero et al., 2015c).

**Prevention Instead of Treatment.** This process opens the possibility to valorise a by-product. The manuscript provides the characterization of the products and discuss the possible application.

**Design for Separation.** Sample eluent can be sent to the filters for liquid and solids separation. The liquid eluent can be further sent to the flash separator for further concentration. The separation steps require no extra energy.

**Maximize Efficiency.** Mass transfer is the limiting step in the biomass fractionation process (Cocero et al., 2018). SCW improve the mass transfer as there is no boundary between liquid and gas phase and reaction is conducted in one, SCW phase. This is the key point for process intensification, as reaction time is shorter, under 1s. This result in the low reaction volume required.

**Output-pulled versus Input-pushed.** Zero-petroleum-based society is getting closer. Future legislation is going in that direction. Soon, a great demand of nature-based products will require processes like this one. The liquid effluent from the process could be used for fermentation, producing base products (like ethanol, butanol, etc.), where also compounds with antioxidant activity could be isolated. The solid effluent is enriched in lignin and lignin-carbohydrate complex that could be further refined and potentially used for new plastics. As mentioned above the heat recovery is considered in all the process steps (Cantero et al., 2015c).

**Conserve complexity.** The innovative process proposed allows for the quick disintegration of biopolymers. The control of the reaction time and reaction conditions allows high yield and selectivity toward desired products (Abad-Fernández et al., 2019; Cantero et al., 2013; Martínez et al., 2015). The operation at high P and T is an opportunity for heat integration (Cantero et al., 2015c).

**Durability rather than immortality.** The process can operate with different feedstocks, as different biomasses or biopolymers. This brings high diversity of obtained products that are nature based, so that they can be durable but also biodegradable. The plant and devices used are improved with new materials that support operation at high pressures and temperatures.

**Meet need, minimize excess.** Reaction time is one of the main variables that influence the selectivity of the process (Cocero et al., 2018). The reaction time can be easily adjusted just by changing the length of the reactor or the flow of biomass and water streams. Innovative Sudden-expansion micro-reactor (SEMR) supported in a tubular reactor concept allow to operate with residence time from 0.1s.

**Minimize material diversity.** Innovative reactor design supported in conventional high-pressure devices is accessible and disassembly friendly.

**Integrate material and energy flows.** The process energy demand considers the heat recovery from the effluent to the SCW preheaters. The heat integration developed allow the recovery of effluent work and heat

(Cantero et al., 2015c).

**Design for commercial “afterlife”.** SCWH process is a continuous process easy to scale up (Martínez et al., 2019). A Demo plant is running for production of commercial products (<https://renmatix.com/>, n.d.). The production is very flexible due to the possibility of obtaining wide range of products when biomass feedstock is changed or/and operating conditions.

**Renewable rather than depleting.** The grape seeds are a renewable material source, and the thermal and electrical energy can be easily produced from the renewable source too.

## 2. Experimental

### 2.1. Materials

Defatted grape seeds were provided from Alvinesa Natural Ingredients (Spain). The grape seeds were defatted using hexane-extraction. Deionized water was used as the reaction medium. The HPLC standards (cellobiose, galacturonic acid, glucuronic acid, glucose, mannose, xylose, fructose, arabinose, glyceraldehyde, glycolaldehyde, lactic, formic, acetic and acrylic acids, furfural and 5-hydroxymethylfurfural (5-HMF)) were purchased from Sigma Aldrich, as well as sulfuric acid and calcium carbonate for biomass characterization. For Kjeldahl determination of protein content, Kjeldahl catalyst (0.3 % CuSO<sub>4</sub>·5H<sub>2</sub>O) tablets were purchased from PanReac. Dioxane was used for extraction of lignins from the sample's solid phase and deuterated dimethyl sulfoxide (DMSO-*d*<sub>6</sub>) as solvent for 2D NMR analysis.

### 2.2. Methods

#### 2.2.1. Biomass and sample characterization

Prior to SCWH defatted grape seeds were ball milled using Retsch equipment, for 4 h. The composition was characterized using the Laboratory Analytical Procedure (LAP) of the National Renewable Energy Laboratory (NREL) (Hames et al., 2008; A Sluiter et al., 2008b, 2008c; A. Sluiter et al., 2008). After the SCWH the sample was obtained as suspended solid and further centrifuged for 10 min at 7800 rpm and then separated to liquid and solid phase. The solid phase was dried at 50 °C and further analysed. The composition of solid and liquid phase was analysed by LAP procedures. For analysis of the solid phase the procedure for determination of structural carbohydrates and lignin was used (A. Sluiter et al., 2008), while for the liquid phase the procedure for determination of sugars, by-products and degradation products was utilised (A Sluiter et al., 2008a).

The analytical techniques used in biomass and sample characterization are described as follows.

**High Performance Liquid Chromatography** analysis using Shodex SH-1011 column for components separation at 50 °C and sulfuric acid (0.01 N) as the mobile phase with a flow rate of 0.8 mL/min. A RI-detector (Waters 2414) was used to identify the sugars and their derivatives. The sample was prepared using the before mentioned LAP procedures.

**Total Organic Carbon** was analysed in the liquid phase of the sample using Shimadzu TOC-VCSH.

**Elemental analysis** of the sample's solid phase was performed in order to determine carbon, hydrogen, nitrogen and sulfur content using Elemental C-S analyser with a Leco CS-225.

**Fourier-Transform Infrared Spectroscopy (FT-IR)** was utilised to follow the structural changes in biomass before and after hydrolysis using Bruker Tensor 27. The recorded spectra were baseline-subtracted and normalized to the maximum peak intensity. Each processed spectrum was hereby a mean of 64 single scans. The sample was analysed without further preparation.

**UV-VIS Spectroscopy** was used to determine the total amount of soluble lignin after acid hydrolysis of biomass and solid sample. The absorbance was recorded at a wavelength of 280 nm, using an

absorptivity coefficient of 17.08 L g<sup>-1</sup>cm<sup>-1</sup>.

**Scanning Electron Microscopy (SEM)** experiments were conducted in a Hitachi FlexSEM 1000 to determine morphological changes on the sample surface.

**Differential Scanning Calorimetry (DSC)** was used to determine glass transition temperature of lignin in biomass and solid samples. The used device was a Mettler Toledo DSC 3+.

#### 2.2.2. Milled wood lignin and dioxane-lignins preparation and characterization

For Milled Wood Lignin (MWL) isolation, a classical method was used (Björkman, 1956) with modifications described by Balakshin et al. (2011). 4 g of defatted grape seeds were milled for 8 h in a jar of 80 mL volume by using 34 balls of ZrO<sub>2</sub>. The diameter of each ZrO<sub>2</sub> ball is 10 mm. 15 min break has been used after each 30 min of milling to keep the temperature of the biomass below 50 °C. Obtained meal was extracted with dioxane (96% v/v) and the solvent was then evaporated under vacuum at 35 °C. Obtained solid was dried in a vacuum oven at 40 °C to obtain MWLs preparations.

The supercritical water lignins were isolated by dioxane extraction, following a procedure described earlier (Capanema and Balakshin, 2015).

**2D Nuclear Magnetic Resonance Spectroscopy (2D-NMR)** was conducted using a Bruker Avance 600 NMR with a magnetic flux density of 14.1 T and equipped with a cryogenically cooled 5 mm TCI probe head with inverse geometry (i.e., optimized for proton signal detection). A total of 36 transients (scans per block) were acquired using 1024 data points in the F2 (1H) dimension for and acquisition time of 77.8 ms and 256 data points in the F1 (13C) dimension for an acquisition time of 3.94 ms. The 2D data set was processed with 1024 × 1024 data points using the Qsine function in both dimensions. The sample was prepared for 2D-NMR by dissolving approximately 70 mg of lignin in 0.6 mL of DMSO-*d*<sub>6</sub>.

#### 2.2.3. Supercritical water hydrolysis pilot plant

A description of the operating details and procedure of the ultrafast SCWH Plant can be found in the previous work of our research group, in addition to a discussion of scaling up the process from laboratory to pilot plant (Martínez et al., 2019). Briefly, the design of the plant provides short reaction times due to the small reactor volume and a fast flow through the reactor. The instantaneous mixing of biomass and SCW in the T junction, just in the inlet of the reactor, allows avoiding all degradation reactions that could occur during the heat-up. A valve for high temperature and pressure conditions is based at the end of the reactor. This provides a decrease in temperature of the sample stream down to 150 °C, caused by the Joule-Thomson effect. Due to this immediate temperature decrease all reactions are stopped. Regarding that one of the determining factors of hydrolysis is reaction time, its precise control is enabled by the design of the plant, simply by changing the length of the reactor or total flow. The reactor geometry and high flow rates provide a turbulent flow and thus ensure good mixing. The maximum operating conditions of the plant are 450 °C and 300 bar with a maximum capacity 40 kg h<sup>-1</sup> of biomass suspension. The flow diagram of the plant is presented in Fig. 1.

Defatted grape seeds were hydrolysed in SCW at 380 °C and 260 bar for different reaction times, ranging from 0.18 s to 1 s, with maximum biomass flow of 4.9 kg h<sup>-1</sup>. The average fluctuation in experiments was around ±2 °C in terms of temperature and ±5 bar in terms of pressure. The reaction temperature of 380 °C in the experiment was the same as the temperature in previous experiments with wheat bran, while in experiments with sugar beet pulp the temperature was 390 °C. Due to high recalcitrance of grape seeds a longer reaction time of up to 1 s was chosen, compared to the reaction time regarding wheat bran and sugar beet pulp hydrolysis (maximum reaction time of 0.17 s in lab scale plant).

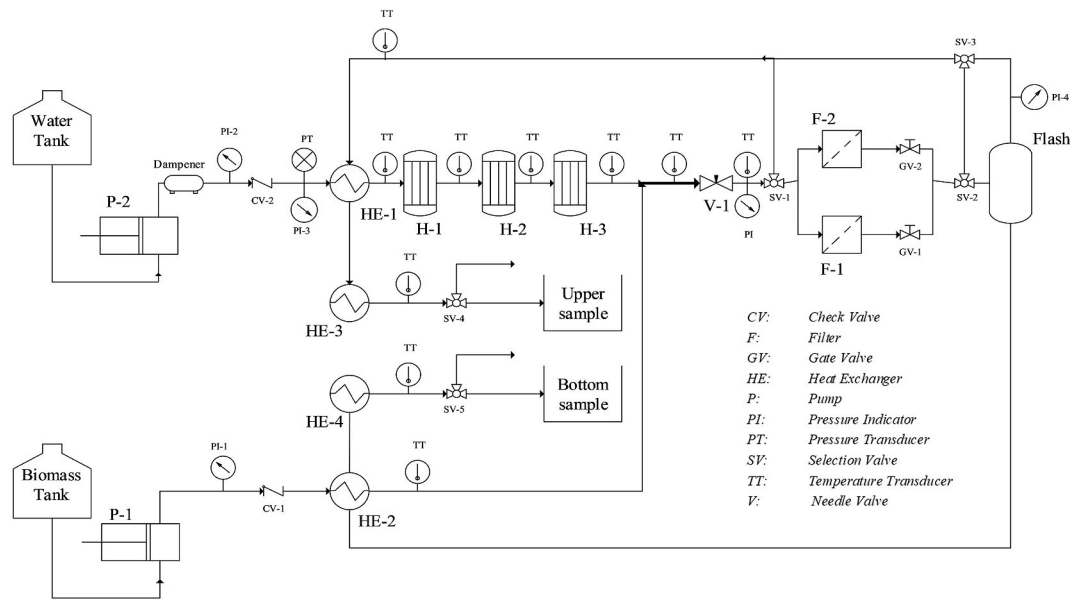


Fig. 1. Ultrafast Supercritical Water Hydrolysis Pilot Plant. SEMR reactor detail.

### 3. Results and discussion

#### 3.1. Biomass characterization

The composition of the biomass as raw material is given in Table 1. This biomass is characteristic for a high lignin content that presents almost half of the biomass structure. As mentioned in the methods section, the biomass was firstly ball milled prior to the hydrolysis and as such characterized. The resulting particle size of the ball milled biomass was 180  $\mu\text{m}$ . Reduction of particle size is necessary in the process due to possible pumping issues as particles with big diameter can cause plugging of the biomass line. This counts especially in the case of defatted grape seeds as a biomass with high lignin content and rigid structure. For the determination of extractives, water and ethanol were used (consequently) as solvent.

#### 3.2. Carbohydrate recovery from the sample liquid phase

After SCW hydrolysis sample was centrifugated so that two phases, liquid and solid, were separated and analysed. The liquid phase was subjected to the acid hydrolysis adding 72% sulfuric acid and diluting the acid concentration to 4%. The sample was then hydrolysed in autoclave for 1 h at 121  $^{\circ}\text{C}$ . During the SCWH process the cellulose and hemicellulose fractions are firstly hydrolysed to oligomers, from oligomers to monomeric sugars and from monomers converted into further degradation products. Acid hydrolysis of the sample is necessary in order to bring oligomeric sugars into monomeric sugars that can be further analysed and quantified. The carbohydrate fractions C6 (glucan)

and C5 (arabinan and xylan) in the biomass, used for sugar yield calculation were obtained using the biomass without previous Soxhlet extraction. Hydrolysable base for sugars was calculated following eq. (1), where  $c_{HS}^C$  is the concentration of hydrolysable to sugars in ppm of carbon,  $c_C^{in}$  is the concentration of carbon inside the reactor in ppm and  $W_{C6}^{biomass}$  and  $W_{C5}^{biomass}$  are the weight fractions of C6 and C5 carbohydrates referring to the biomass in % w/w.

$$c_{HS}^C = c_C^{in} \cdot \left( \frac{W_{C6}^{biomass} + W_{C5}^{biomass}}{100 \% \text{ w/w}} \right) \quad (1)$$

The yield of total sugars ( $Y_{TS}$  in % w/w) was calculated in eq. (2) dividing the concentration of total sugars expressed in ppm of carbon ( $c_{TS}^C$ , see eq. (3)), that was determined in the liquid phase of the sample by HPLC analysis, by the concentration of hydrolysable to sugars ( $c_{HS}^C$ ).

$$Y_{TS} = \frac{c_{TS}^C}{c_{HS}^C} \quad (2)$$

$$c_{TS}^C = c_{C5}^{Cout} + c_{C6}^{Cout} \quad (3)$$

The yields of each sugar fraction ( $Y_{C5}$  and  $Y_{C6}$  in % w/w) were calculated independently, dividing the concentrations of C5 and C6 sugars ( $c_{C5}^{Cout}$  and  $c_{C6}^{Cout}$ ) determined in the liquid by the inlet concentrations of C5 and C6 carbohydrates fraction respectively (eq. (4) and (5)) (both concentration presented with respect to carbon).

$$Y_{C5} = \frac{c_{C5}^{Cout}}{c_C^{in} \cdot W_{C5}^{biomass}} \cdot 100 \% \quad (4)$$

$$Y_{C6} = \frac{c_{C6}^{Cout}}{c_C^{in} \cdot W_{C6}^{biomass}} \cdot 100 \% \quad (5)$$

Carbohydrate fractions are considered as the liable fractions that undergo rapidly the hydrolysis in SCW. By Fig. 2, that present the yield of total sugar in the liquid phase ( $Y_{TS}$ ), it is shown that the highest yield was obtained for a short reaction time of 0.27 s, reaching 61%. Martinez et al. and Cantero et al. showed that the maximum yield of sugars for the hydrolysis of sugar beet pulp and wheat bran were obtained for even shorter reaction times (0.11 s and 0.19 s respectively), operating in a laboratory scale plant (Cantero et al., 2015b; Martínez et al., 2019). The recovery of sugars in the Supercritical water process is higher compared to work reported by Prado et al (Prado et al., 2016), where up to 40%

Table 1

Compositional analysis of defatted grape seeds.

Substance	Composition (% w/w)
Ash	1.9 $\pm$ 0.5
Moisture	8.4 $\pm$ 0.05
Water extractives	12.7 $\pm$ 1.6
Ethanol extractives	2.7 $\pm$ 0.2
Proteins	3.2 $\pm$ 0.2
Acid Insoluble Lignin	36.5 $\pm$ 1.1
Acid Soluble Lignin	6.0 $\pm$ 0.4
Glucan	12.1 $\pm$ 0.12
Xylan	7.6 $\pm$ 0.2
Arabinan	1.3 $\pm$ 0.4

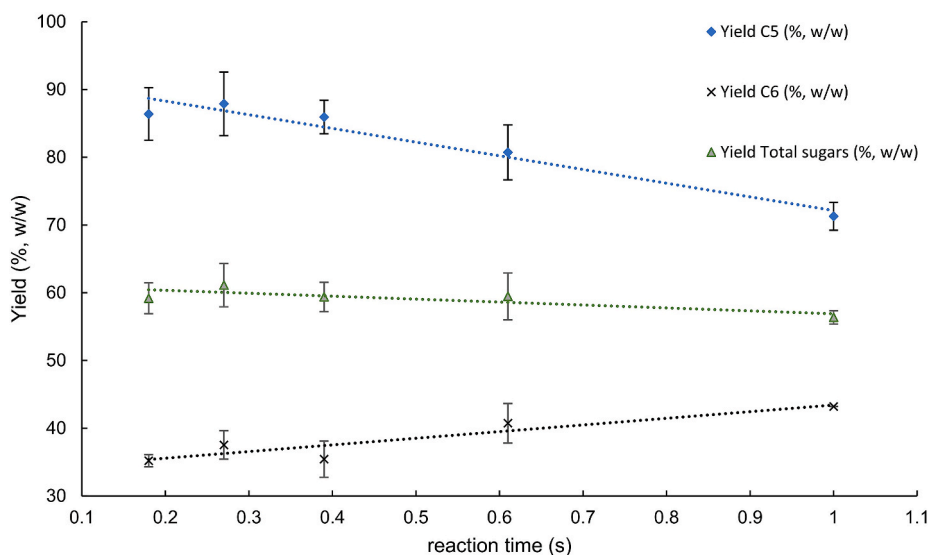


Fig. 2. Yield of C5, C6 and total sugars over reaction time in the liquid phase; the error bars are the standard deviations; linear trendlines given.

sugar was recovered from defatted grape seeds using Subcritical water hydrolysis, under 203 °C–258 °C, 20 MPa for 30 min.

Differently from the case of sugar beet pulp (Martínez et al., 2018), where within 1 s of reaction time the main part of the carbohydrate fractions was already converted and the yield of sugars in the liquid phase rapidly decreased, the yield of the sugar in the case of grape seeds remained high (56%). One of the natural factors that influence biomass recalcitrance is the amount of lignin and other polyphenols. The explanation for slower gradual conversion of the carbohydrate fractions can lie in the high lignin content of the biomass. Lignin could act as a barrier for SCW to access the carbohydrate fractions, as some part of cellulose is less accessible in the inner structure of lignin (Cantero et al., 2015b). The C5 conversion was higher than that of C6. The C5 yield dropped from maximum value of 88% obtained for 0.27–71% for 1s. The maximum yield of C6 sugars was 43% obtained after 1 s.

### 3.3. Solid fraction characterization

The solid yield ( $Y_{solid}$  in % w/w) is calculated by eq. (6), where  $c_{SS}$  is the concentration of suspended solid in the sample in ppm and  $f_C^{solid}$  is the solid carbon factor obtained with elementary analysis of the solid.

$$Y_{solid} = \frac{c_{SS} \cdot f_C^{solid}}{c_C^n} - 100 \quad \% \quad (6)$$

The yield of the solid fraction (see Fig. 3.) decreases with reaction time up to 0.61 s. To obtain higher rates of liquefaction, more severe conditions were needed, decreasing the yield from 60% for a reaction time of 0.18 s–46% for the time of 0.61 s. Slight increase of the solid yield fraction for the longest reaction time of 1s could be result of the production of the water insoluble compound as the reaction proceeds.

Solid characterization by LAP procedure for carbohydrate and lignin content is presented in Fig. 4. It is important to note that extractives were not removed from the solid sample and that they could contribute to the total amount of the Klason lignin. The amount of carbohydrates and lignin fractions in biomass presented in Fig. 4 is also calculated for the biomass as received, without previous extraction. As carbohydrate fractions are more labile fractions, they undergo to hydrolysis fast while the amount of acid insoluble solid increased in the solid fraction for already shortest reaction time, to 61%, and goes to 65% for the longest reaction time. As mentioned above the biomass' high content of insoluble lignin increases its recalcitrance and reacts as barrier to total hydrolysis of sugars fraction, as even for the longest reaction time of 1 s,

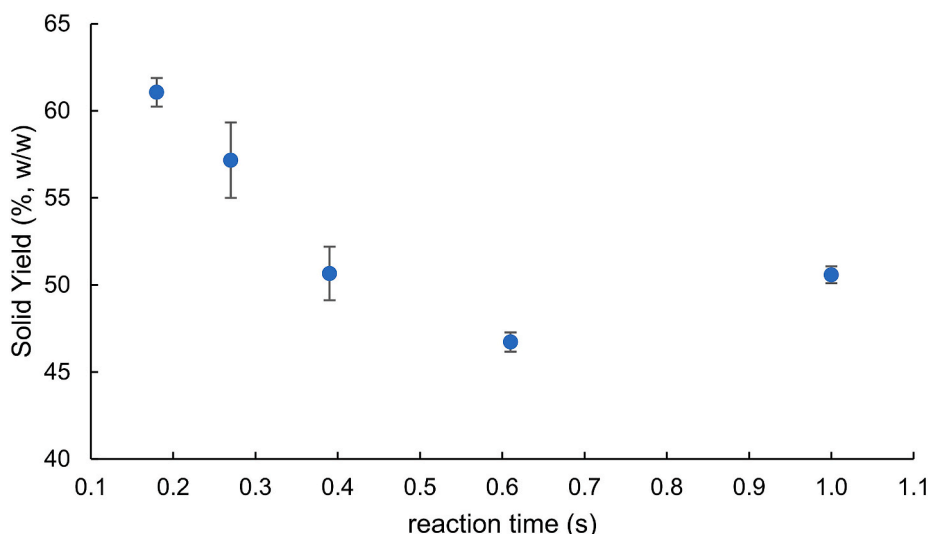
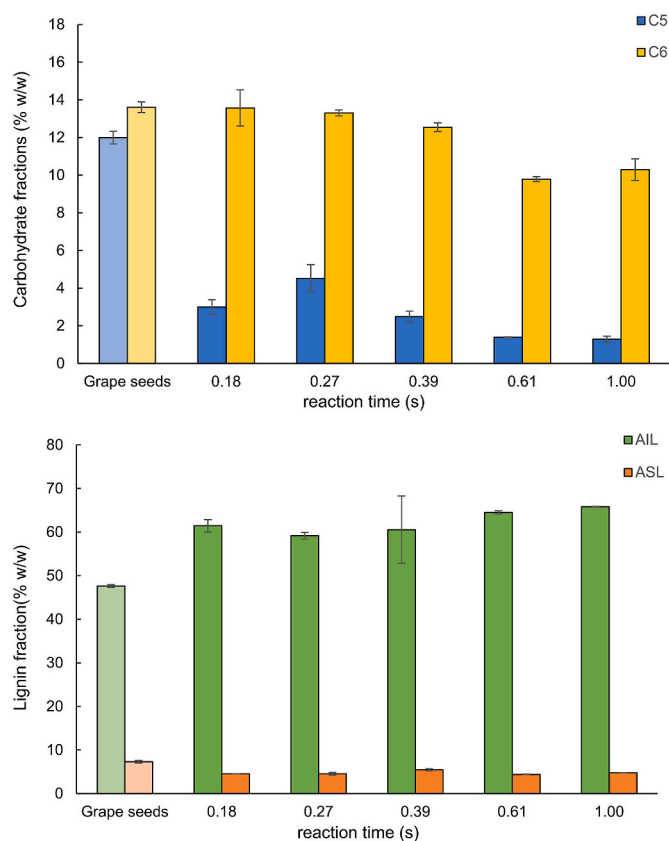


Fig. 3. Yield of solid after SCWH over reaction time.



**Fig. 4.** Solid sample composition over reaction time; top: carbohydrate fractions (where C6 refers to glucose and C5 to sum of xylose and arabinose); bottom: acid insoluble lignin (AIL) and acid soluble lignin (ASL).

the solid phase still contained 10% of the carbohydrates fraction. This is different compared to the biomass composed mainly of the more labile fractions as above-mentioned sugar beet pulp (Martínez et al., 2018) as for this biomass high recovery of sugars was obtained in the liquid

phase, and just 0.9% of carbohydrates fraction was determined in solid phase after similar reaction time.

FT-IR signals for raw biomass and solids for different times (0.18 s, 0.39 s, 0.61 s) are presented on Fig. 5 and assign according to the literature (Ehara et al., 2005; Hemmilä et al., 2020; Sahoo et al., 2011; Wahyudiono et al., 2008; Xu et al., 2013). The FT-IR signals of solids after hydrolysis showed increased intensity in the region related to lignin structure approving the increased aromaticity of the solid after the process. The increased intensity was observed for peaks at: 779  $\text{cm}^{-1}$  assigned to C-H out of plane vibration on the aromatic ring; 1270  $\text{cm}^{-1}$  assigned to the guaiacyl ring breathing and C=O stretching; 1315  $\text{cm}^{-1}$  assigned to aromatic ring breathing; 1617  $\text{cm}^{-1}$  and its shoulder at 1650  $\text{cm}^{-1}$  assigned to the aromatic ring vibration of phenylpropane groups and C=O bonds in conjugated ketones; 3430  $\text{cm}^{-1}$  assigned to O-H stretching specifically from lignin. Peak at 1050  $\text{cm}^{-1}$  assigned to the C-O-C ether linkage of the skeletal vibration of both pentose and hexose unit from hemicellulose and cellulose decreased due to the hydrolysis of carbohydrate structures in the solid residue.

Reported Glass Transition Temperature ( $T_g$ ) for different underivatized lignin lies between 90 and 180  $^{\circ}\text{C}$  (Daz et al., 2001). The DSC curves for the biomass sample and solid after SCWH at reaction times of 0.18 s, 0.39 s and 0.61 s are shown in Fig. 6. The biomass sample shows a peak that could correspond to the lignin transition temperature at 152  $^{\circ}\text{C}$ , while the solid obtained after reaction times of 0.18 s, 0.39 s and 0.61 s have peaks shifted to higher temperature, 162  $^{\circ}\text{C}$ , 165  $^{\circ}\text{C}$  and 167  $^{\circ}\text{C}$  respectively, that is higher compared to other lignins. The results in the literature report that the same molecular motion of in situ lignin has been observed at the temperature lower than that of the isolated lignin and that shifted  $T_g$  suggests that the amorphous structure of lignin could be affected by coexisting components in the original biomass, but also by mechanical and thermal changes during the treatment (Hatakeyama et al., 2010). Higher  $T_g$  values of lignin obtained after processing, even increased with the severity of the process. Determination of  $T_g$  value is an important information for potential application of lignin.

At temperatures above 250  $^{\circ}\text{C}$  peaks that correspond to the degradation of main constituents of samples, hemicellulose, cellulose and lignin, can be observed. These peaks can be seen in the region of 285  $^{\circ}\text{C}$ –296  $^{\circ}\text{C}$  for hemicellulose, 347  $^{\circ}\text{C}$ –360  $^{\circ}\text{C}$  for cellulose and 402  $^{\circ}\text{C}$ –417  $^{\circ}\text{C}$  for lignin. Similar degradation temperatures of main

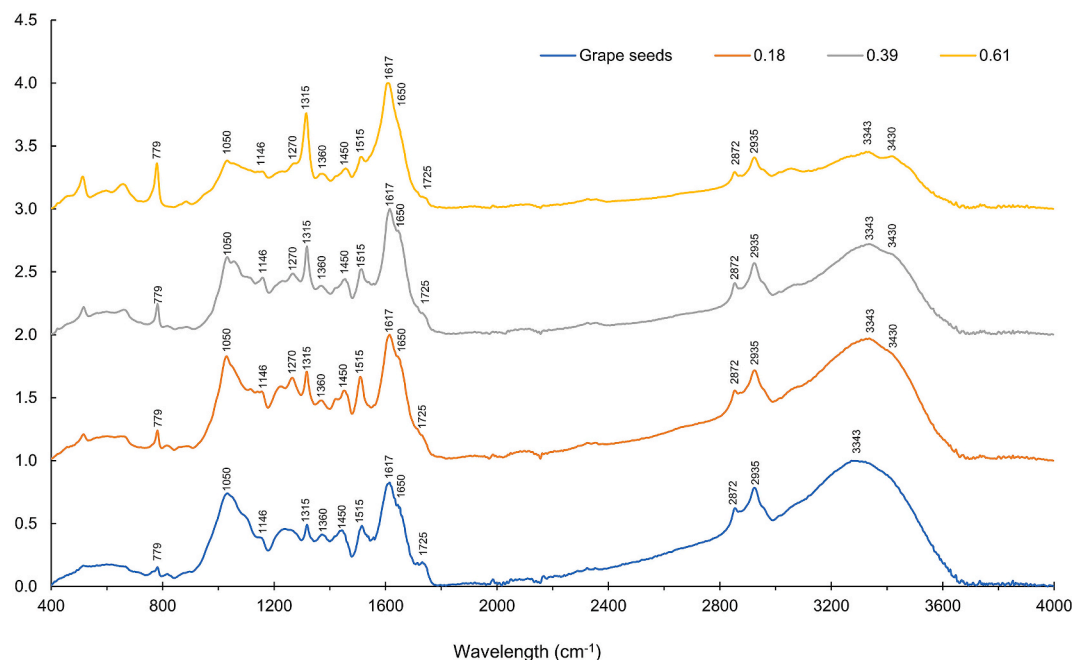


**Fig. 5.** FT-IR spectrum of raw material and solid after hydrolysis at 0.18 s, 0.39 s and 0.61 s.

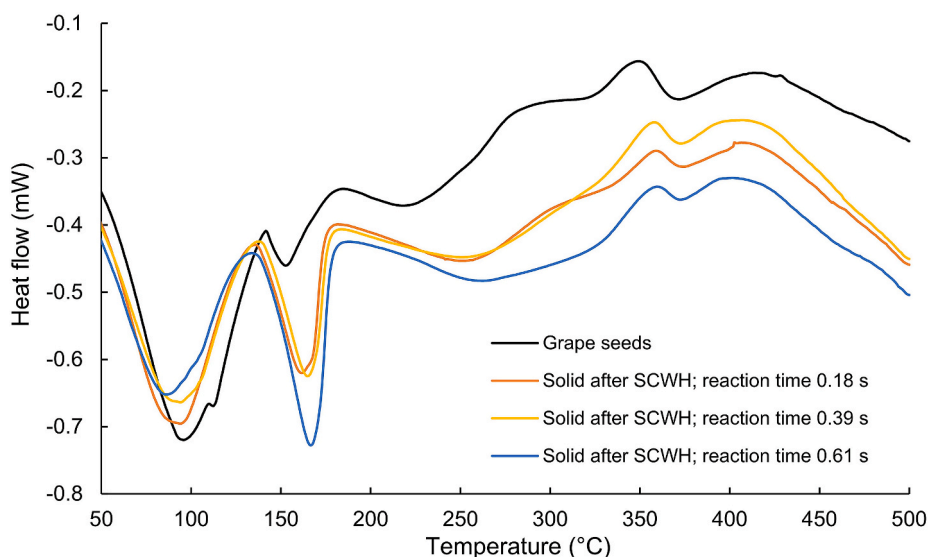


Fig. 6. DSC curves for raw biomass and solid after SCWH for reaction times of 0.18 s, 0.39 s and 0.61 s.

biomass constituents obtained by DSC analysis were reported by Brys et al. when different wood species were analysed (Brys et al., 2016). For the SCWH sample obtained after 0.61 s, the peak that corresponds to hemicellulose degradation was almost absent, as the main amount of hemicellulose was already hydrolysed. The peak that corresponds to cellulose degradation was observed at 347 °C for GS, while for SCWH solids this peak was at 359 °C, 356 °C and 360 °C (for 0.18 s, 0.39 s, 0.61 s respectively). The higher degradation temperature of cellulose in solids after SCWH compared to GS might be due to the more crystalline structure of the cellulose that remained in the solid, as a more labile amorphous part is firstly hydrolysed, or due to the part of cellulose chemically bonded to lignin polymer. The highest degradation temperatures correspond to lignin, as lignin is the most thermostable constituent of biomass (Brys et al., 2016). Due to the complexity of the lignin structure, its thermal degradation happened over a wide temperature range (Yang et al., 2007).

SEM analysis was performed for solid obtained at different reaction times in order to observe changes in morphology of biomass caused by hydrolysis and severity of the process (Fig. 7). The sample before hydrolysis had a compact surface structure, while the influence of the SCWH clearly causes structural damage. These ruptures are more visible with longer reaction times. The surface of treated solid also shows appearance of the small droplets that can be related to the molten lignin

at high temperature and pressure (Donohoe et al., 2008; Kristensen et al., 2008; Pingali et al., 2010; Selig et al., 2007; Xiao et al., 2011). This is in accordance to compositional analysis of solid fraction, as it is mainly composed of lignin. Since lignin plays a significant role in biomass recalcitrance this can be the reason for a slower rate of carbohydrate hydrolysis in SCW, compared to the biomass with a lower amount of lignin as explained above. Lignin is also specific to be relocated during the hydrothermal treatment, so that upon melting, lignin in biomass becomes fluid and thus can move through the cell wall matrix observed as spherical formations on the surface of pre-treated biomass (Selig et al., 2007). He et al. assign appearance of aggregated droplets to pseudo lignin that originate from the condensation and aromatisation reaction of sugar degradation products during dilute acid pre-treatment (He et al., 2018). The released aromatic compounds from lignin degradation also have effect of the formation of pseudo lignin that have polyaromatic phenolic nature and contribute of the total amount of Klason lignin (He et al., 2020).

#### 3.4. Structural analysis of grape seed MWL and extracted polyphenols mixture by 2D NMR

The supercritical water process produces solid enriched in lignin. This solid can be further refined to obtain a higher purity of lignin,

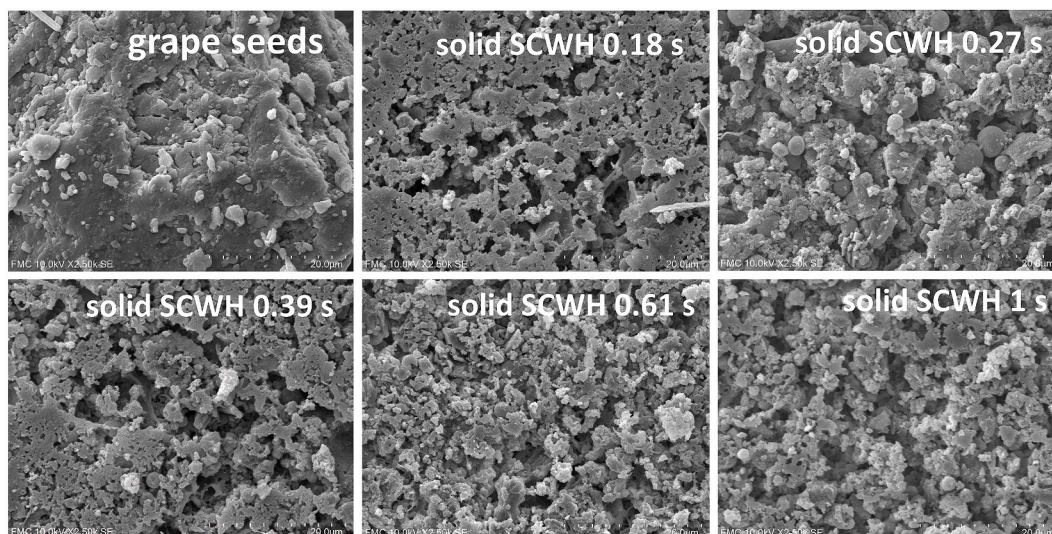


Fig. 7. SEM images of raw material and solids after SCWH obtained for different reaction times (0.18 s, 0.27 s, 0.39, 0.61 s and 1 s).

named as SCWL in text below (Capanema and Balakshin, 2015). For structural characterization with high-resolution NMR, lignins (with chemically linked carbohydrates) were extracted from the solids after SCWH with 80% v/v dioxane. This solvent mixture allows about

maximal solubility of lignin and LCC components (Balakshin et al., 2003) without possible chemical modification. This counts for instances in the case of NaOH extraction, especially for a very complex non-wood plant biomass containing significant amounts of ester and other labile moieties (e.g., polyphenols). The extraction yield (dioxane lignin) was about 55–57% w/w per lignin content in the solids obtained after SCWH.

The extracted SCWL were analysed by a HSQC 2D NMR method (shown in Fig. 8), to obtain information on changes that occur in lignin structure during the hydrolysis process. The MWL isolated from grape seeds feedstock was used for comparison, as MWL is considered to be relatively close to the native lignin structure (Balakshin et al., 2020b). Table 2 presents the assignments of main lignin cross-peaks and their quantification in the spectra of MWL and SCWL isolated after reaction times of 0.18 s, 0.27 s and 0.39 s.

The spectra (see Fig. 8) show clearly that the extracted SCWL are very complex mixtures of different types of chemicals, such as lipophilic extractives, polyphenols (e.g., flavonoids) and true polymeric lignin, which is also linked to carbohydrates via chemical linkages. Detailed analysis of the SCWL is extremely challenging due to the high complexity of the mixture and significant signals overlap even in the 2D spectra. Therefore, only high-level conclusions are possible at the current stage.

Lignin from grape seeds consisted mainly of G type units, with minor amount of H units, while S units were practically absent. Main lignin signals were assigned according to the literature available (Balakshin et al., 2003, 2011; Lancefield et al., 2018). Apart of main lignin units the 2D NMR data shows the presence of lignin – carbohydrate linkages, i.e., the presence of Lignin Carbohydrate Complex (LCC). Three types of LCC linkages, namely benzyl ether (BE), phenyl glycoside (PhGlc) and  $\gamma$ -ester were detected ( $\delta_C/\delta_H$  79.6–82.8/4.4–4.9, 99.4–103.7/4.8–5.1 and 60.8–62.9/4.2–4.4, respectively). Importantly, other BE (lignin-lignin) and esters moieties can also contribute to these resonances (Balakshin et al., 2011, 2014, 2020b), therefore they show only maximal possible amounts of LCC linkages. In addition, high varieties and high amounts of lipophilic extractives and flavonoids were detected in the spectra. Lignin from grape seeds differs from lignin isolated from the grape stalks, as the latter contains significant amount of S units that were not found in the grape seeds MWL. Condensed structures of alkyl-aryl type were also determined in the lignin from grape stalks, and they are at least partially, assigned to the lignin–tannin condensed structures (Prozil et al., 2014).

For a semiquantitative analysis, the resonance of methoxyl groups was used as a reference to normalize the resonance values of the other

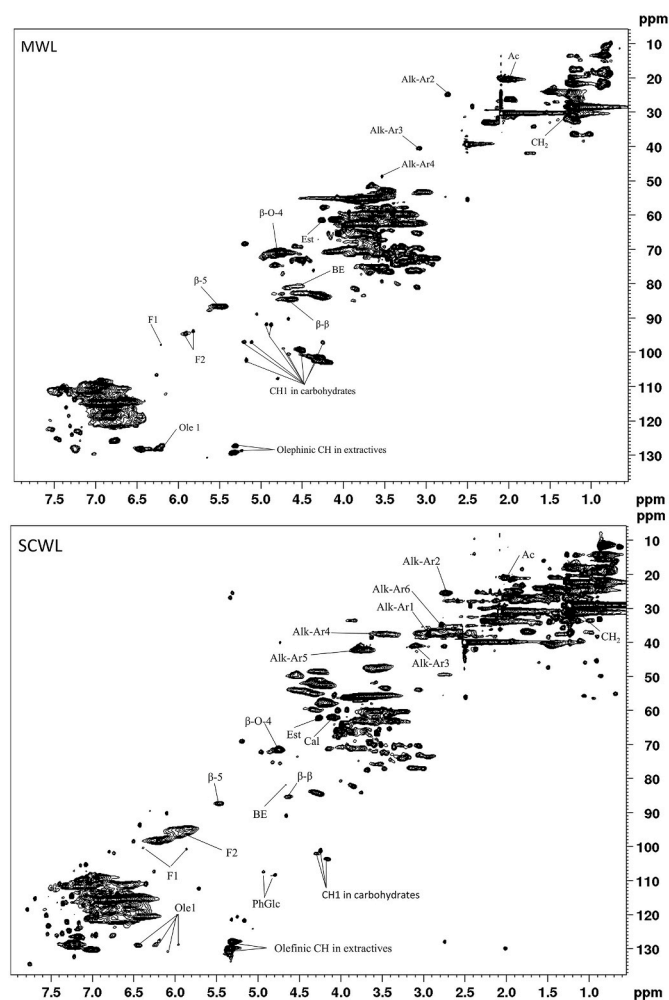


Fig. 8. HSQC spectra; top: milled wood lignin; bottom: SCWL (at reaction time of 0.39 s).

Table 2

Relative amounts of different moieties of milled wood lignin (MWL) and supercritical water lignins (SCWL) at different reaction times (0.18 s, 0.27 s and 0.39 s).

$\delta_C/\delta_H$	MWL	0.18 s	0.27 s	0.39 s	assignment
69.3–73.6/4.6–5.0	33.9	26.0	26.7	24.4	$\beta$ – aryl ether ( $\beta$ -O-4)
84.0–86.0/4.5–4.8	6.7	4.7	5.3	4.8	resinol ( $\beta$ - $\beta$ )
86.1–88.5/5.4–5.6	10.3	7.8	7.6	6.9	phenyl-coumaran ( $\beta$ -5)
60.7–62.9/4.0–4.2	14.4	14.9	17.8	16.5	coniferyl alcohol (Calk)
60.8–62.9/4.2–4.4	3.4	5.6	9.1	6.4	$\gamma$ – esters (Est)
79.6–82.8/4.4–4.9	7.5	12.8	12.6	11	benzyl ethers (BE)
99.4–103.7/4.8–5.1	4.1	2.0	0.5	1.4	Phenyl glycosides (PhGlc)
19.2–22.0/1.8–2.1	32.4	43.4	26.1	38.6	Acetyl groups (Ac)
97.0–100.5/5.8–6.4	1.7	35.5	35.0	38.8	Flavonoids (F1)
93.6–96.9/5.7–6.3	6.7	55.3	49.4	35.0	Flavonoids (F2)
98.9–105.1/4.0–4.8	28.4	17.5	7.3	13.1	CH1 in carbohydrates
35.9–39.2/2.9–3.0	1.1	14.2	11.0	22.5	Alkyl-Aryl moieties (Alk-Ar1)
23.2–26.3/2.6–2.8	2.3	50.6	69.4	60.8	Alk-Ar2
39.6–43.9/3.0–3.2	1.6	20.9	11.9	10.1	Alk-Ar3
35.4–39.6/3.3–3.7	0.8	23.3	21.0	24.8	Alk-Ar4
45.5–49.3/3.4–3.8	1.9	36.3	30.4	34.0	Alk-Ar5
39.9–44.9/3.6–3.9	1.9	64.3	27.9	42.9	Alk-Ar6
33.4–36.3/2.7–2.9	0.7	7.0	5.8	11.9	Alk-Ar6
125.6–133.2/5.8–6.5	16.8	30.3	24.5	29.5	Olefinic 1
133.2–150.8/7.1–8.2	4.7	19.7	17.9	23.3	Olefinic 2
27.7–33.1/1.0–1.3	120.3	748.4	1043.6	972.3	CH2 (mainly extractives)
125.9–133.9/5.1–5.5	8.7	149.2	192.8	180.8	olefinic CH in extractives



signals. It was set as 300 to express the value obtained close to 100 lignin monomeric units (i.e. expressed in mol % in respect to lignin). A more common approach (for lignins) using resonance of G2 cannot be used in our case as it is obscured with the resonance of non-lignin signals, apparently flavonoids. Very approximate calculation shows that lipophilic extractives, flavonoid and lignin are present in a similar mass proportion, i.e. lignin share in the extracted material is about 30–40% w/w. In terms of advanced biorefinery, these valuable components might be further fractionated (if they are not linked chemically) e.g., by solvents of different polarities or/and other manners. Alternatively, the effect of the presence of non-lignin compounds and potential synergism of them (Balakshin et al., 2020a), in typical lignin application may be also studied in terms of advanced biorefinery.

There is no clear tendency in the amounts of lipophilic extractives and flavonoids in the dioxane extracts of SCWL during the reaction course. The amounts of these components in MWL are dramatically less as the biomass was pre-extracted with toluene-ethanol prior to lignin isolation according to the classical procedure (Balakshin et al., 2011) indicated that they are not chemically linked to lignin in the original biomass. In contrast, the amounts of residual LCC (evaluated by the amounts of carbohydrates in the samples) was lower in the SCWL indicating cleavage of LCC linkages during the SCWH. Interestingly, the amounts of ester and BE moieties do not correlate with the amount of carbohydrates in the samples, indicating potential presence of ester and ether linkages of different types (e.g., acetyl groups, lignin-lignin ethers etc). Notably, the amount of labile acetyl groups (from carbohydrates and/or lignin) does not decrease during SCWH.

The amounts of main moieties of native lignin, e.g.,  $\beta$ -O-4,  $\beta$ -5 and  $\beta$ - $\beta$  structures, decrease very slightly during the SCWH process (compare Table 2), at least in the range of 0–0.39 s when the major changes in biomass component separation occur. Such, the content of the main lignin reaction centres,  $\beta$ -O-4 moieties, decrease by only ca 30%. This is in strict contrast to other biorefinery processes when the amounts of  $\beta$ -O-4 linkages decreases by 3–10 times (Balakshin and Capanema, 2015).

Moon et al. reported significant decrease in  $\beta$ -O-4 amount specifically and in the oxygenated aliphatic moieties in general after SCWH but under much severe process conditions (380 °C and 60 s), which sound very unreasonable in the light of our results. They also claim strong demethylation, which however, cannot be justified due to clearly insufficient processing of the  $^{13}\text{C}$  NMR spectra obtained; no

quantification was performed and the spectra were compared at rather different intensities that does not allow any reliable conclusion unless the changes were dramatic (such as decrease in oxygenated aliphatic region) (Moon et al., 2011).

Significant resonance in the saturated aliphatic region of the SCWL, specifically in different moieties of Alkyl-Aryl types, was observed. These signals likely belong to flavonoids of different types. Some lignin condensed moieties also resonate in this region, but their amounts are usually in order of magnitude lower even after significant lignin conversion (Balakshin et al., 2003; Balakshin and Capanema, 2015), which is not the case here. Main lignins' linkages and LCC linkages are given in Fig. 9.

#### 4. Conclusion

Defatted grape seeds were hydrolysed in supercritical water where the recovered yield of sugars in the liquid phase reaches 61% for 0.27 s and solid enriched in polyaromatics is produced. High content of insoluble lignin in grape seeds biomass creates additional mass transfer limitation that acts as barrier to higher recovery of sugars. After longest reaction time of 1 s still 10% of carbohydrates remained in the solid, differently to the result obtained with biomass that has low content of insoluble lignin where almost all carbohydrate fractions could be extracted. Solid phase of the sample consists of a very complex mixture that partially belong to lignin with a certain amount of chemically linked carbohydrates, residual lipophilic extractives and flavonoids. Influence of supercritical water hydrolase on lignin structure was investigated by 2D-NMR analysis that indicates that cleavage of  $\beta$ -O-4 linkages and other native lignin moieties during the supercritical water process are very subtle, that can be beneficial in valorisation of this lignin residue.

#### CRedit authorship contribution statement

**Tijana Adamovic:** main author, Investigation, Methodology, experimental data, Conceptualization, Writing – original draft. **Dmitry Tarasov:** author, NMR, Methodology, & data, Conceptualization. **Emre Demirkaya:** author, Investigation. **Mikhail Balakshin:** author, NMR, Validation, Writing – review & editing. **Maria José Cocero:** corresponding author, Supervision, Conceptualization, Visualization, Validation, Writing – review & editing.

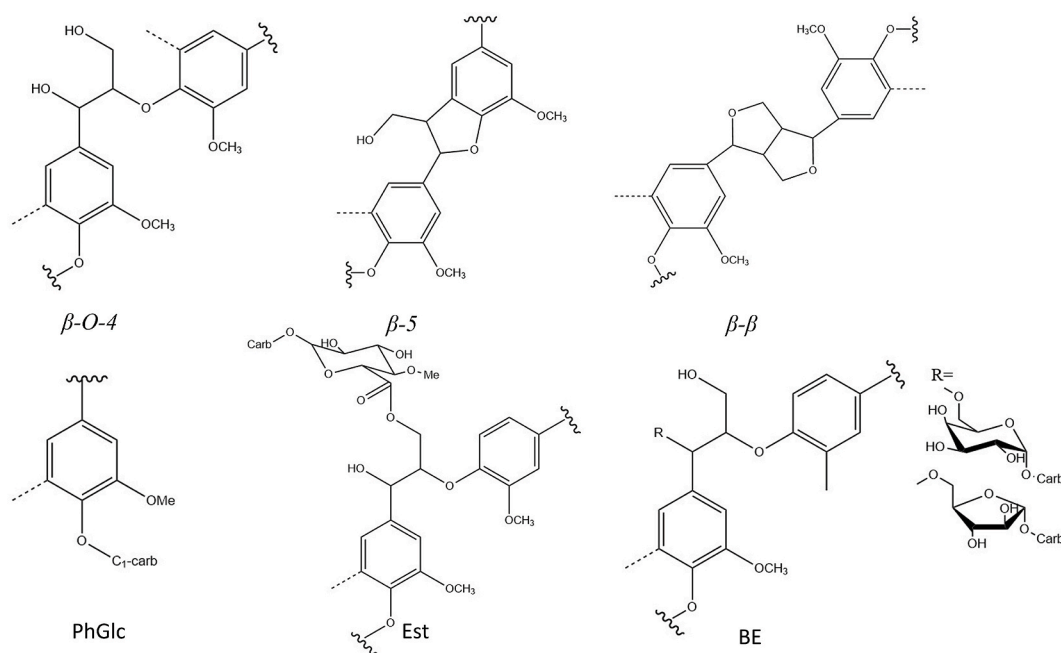


Fig. 9. Main lignin and LCC linkages in Grape seed MWL and SCWL.

## Declaration of competing interest

The authors declare that they have no known competing financial interests or personal relationships that could have appeared to influence the work reported in this paper.

## Acknowledgements

The authors thank the Spanish Ministry of Science & Innovation &

JCyL and European Regional Development Fund for funding the Projects CTQ2016-79777-R & PID2019-105975 GB-I00 & VA277P18. Alvinosa Natural Ingredients (Spain) for supplying us with defatted grape seeds. Tijana Adamovic thanks Valladolid University for FPI UVA Grant. Dmitry Tarasov thanks the FinnCERES flagship program.

## List of symbols and abbreviations

SCW	Supercritical Water
SCWH	Supercritical Water Hydrolysis
SCWL	Supercritical Water Lignin isolated with dioxane
2D NMR	Two-Dimensional Nuclear Magnetic Resonance
SEMR	Sudden-Expansion Micro Reactor
HPLC	High Performance Liquid Chromatography
LAP	Laboratory Analytical Procedure
NREL	National Renewable Energy Laboratory
DMSO- $d_6$	Deuterated Dimethyl Sulfoxide
TOC	Total Organic Carbon
FT-IR	Fourier-Transform Infrared Spectroscopy
UV-VIS Spectroscopy	Ultraviolet-Visible Spectroscopy
SEM	Scanning Electron Microscopy
DSC	Differential Scanning Calorimetry
T <sub>g</sub>	Class transition temperature
LCC	Lignin-Carbohydrate Complex
MWL	Milled Wood Lignin
$C_{HS}^C$	Concentration of hydrolysable to sugars in ppm of carbon
$C_C^In$	Concentration of carbon inside the reactor (ppm)
$W_{C6}^{biomass}$	Fractions of C6 carbohydrates referring to the biomass in % w/w
$W_{C5}^{biomass}$	Fractions of C5 carbohydrates referring to the Biomass in % w/w
$Y_{TS}$	The Yield of Total Sugars
$C_{TS}^C$	Concentration of carbon (ppm) from total sugars
$Y_{C5}$	Yields of C5 fraction (% w/w)
$Y_{C6}$	Yields of C6 fraction (% w/w)
$C_{C5}^{out}$	Concentration of carbon (ppm) from C5 sugars out
$C_{C6}^{out}$	Concentration of carbon (ppm) from C6 sugars out
$Y_{solid}$	The solid yield (% w/w)
$C_{SS}$	Concentration of suspended solid in the sample (ppm)
$f_C^{solid}$	Carbon factor of the solid

## Appendix A. Supplementary data

Supplementary data to this article can be found online at <https://doi.org/10.1016/j.jclepro.2021.129110>.

## References

- <https://renmatix.com/> ([WWW Document], n.d).
- Abad-Fernández, N., Pérez, E., Cocero, M.J., 2019. Aromatics from lignin through ultrafast reactions in water. *Green Chem.* 21, 1351–1360. <https://doi.org/10.1039/c8gc03989e>.
- Anastas, P.T., Zimmerman, J.B., 2007. Design through the 12 principles of green engineering. *IEEE Eng. Manag. Rev.* 35, 16. <https://doi.org/10.1109/EMR.2007.4296421>.
- Aristizábal-Marulanda, V., Chacón-Perez, Y., Cardona Alzate, C.A., 2017. The biorefinery concept for the industrial valorization of coffee processing by-products. In: *Handbook of Coffee Processing By-Products: Sustainable Applications*. Elsevier Inc. <https://doi.org/10.1016/B978-0-12-811290-8.00003-7>.
- Balakshin, M.Y., Capanema, E.A., Chen, C.L., Gracz, H.S., 2003. Elucidation of the structures of residual and dissolved pine kraft lignins using an HMQC NMR technique. *J. Agric. Food Chem.* 51, 6116–6127. <https://doi.org/10.1021/jf034372d>.
- Balakshin, M., Capanema, E., Gracz, H., Chang, H. min, Jameel, H., 2011. Quantification of lignin-carbohydrate linkages with high-resolution NMR spectroscopy. *Planta* 233, 1097–1110. <https://doi.org/10.1007/s00425-011-1359-2>.
- Balakshin, M., Capanema, E., Berlin, A., 2014. Isolation and Analysis of Lignin-Carbohydrate Complexes Preparations with Traditional and Advanced Methods: A Review. *Stud. Nat. Prod. Chem.* 42, 83–115. <https://doi.org/10.16/B978-0-444-63281-4.00004-5>.
- Balakshin, M.Y., Capanema, E.A., 2015. Comprehensive structural analysis of biorefinery lignins with a quantitative <sup>13</sup>C NMR approach. *RSC Adv.* 5, 87187–87199. <https://doi.org/10.1039/c5ra16649g>.
- Balakshin, M., Capanema, E.A., Sulaeva, I., Schlee, P., Huang, Z., Feng, M., Borghei, M., Rojas, O.J., Potthast, A., Rosenau, T., 2020a. New opportunities in the valorization of technical lignins. *ChemSusChem* 1–22. <https://doi.org/10.1002/cssc.202002553>.
- Balakshin, M., Capanema, E.A., Zhu, X., Sulaeva, I., Potthast, A., Rosenau, T., Rojas, O.J., 2020b. Spruce milled wood lignin: linear, branched or cross-linked? *Green Chem.* 22, 3985–4001. <https://doi.org/10.1039/d0gc00926a>.
- Balakshin, M.Y., Capanema, E.A., Sulaeva, I., Schlee, P., Huang, Z., Feng, M., Borghei, M., Rojas, O.J., Potthast, A., Rosenau, T., 2021. New opportunities in the

- valorization of technical lignins. *ChemSusChem* 14, 1016–1036. <https://doi.org/10.1002/cssc.202002553>.
- Björkman, A., 1956. Studies on finely divided wood. Part 1. Extraction of lignin with neutral solvents. *Sven. Papperstidning* 59, 477–485.
- Bravi, M., Spinoglio, F., Verdona, N., Adami, M., Aliboni, A., D'Andrea, A., De Santis, A., Ferri, D., 2007. Improving the extraction of  $\alpha$ -tocopherol-enriched oil from grape seeds by supercritical CO<sub>2</sub>. Optimisation of the extraction conditions. *J. Food Eng.* 78, 488–493. <https://doi.org/10.1016/j.jfoodeng.2005.10.017>.
- Brunner, G., 2014. Reactions of synthetic polymers with water, supercritical fluid science and technology. <https://doi.org/10.1016/B978-0-444-59413-6.00009-1>.
- Bryś, A., Bryś, J., Ostrowska-Ligeza, E., Kaleta, A., Górnicki, K., Głowacki, S., Koczko, P., 2016. Wood biomass characterization by DSC or FT-IR spectroscopy. *J. Therm. Anal. Calorim.* 126, 27–35. <https://doi.org/10.1007/s10973-016-5713-2>.
- Cantero, D.A., Bermejo, M.D., Cocero, M.J., 2013. Kinetic analysis of cellulose depolymerization reactions in near critical water. *J. Supercrit. Fluids* 75, 48–57. <https://doi.org/10.1016/j.supflu.2012.12.013>.
- Cantero, D.A., Bermejo, M.D., Cocero, M.J., 2015a. Governing chemistry of cellulose hydrolysis in supercritical water. *ChemSusChem* 8, 1026–1033. <https://doi.org/10.1002/cssc.201403385>.
- Cantero, D.A., Martínez, C., Bermejo, M.D., Cocero, M.J., 2015b. Simultaneous and selective recovery of cellulose and hemicellulose fractions from wheat bran by supercritical water hydrolysis. *Green Chem.* 17, 610–618. <https://doi.org/10.1039/c4gc01359j>.
- Cantero, D.A., Vaquerizo, L., Mato, F., Bermejo, M.D., Cocero, M.J., 2015c. Energetic approach of biomass hydrolysis in supercritical water. *Bioresour. Technol.* 179, 136–143. <https://doi.org/10.1016/j.biortech.2014.12.006>.
- Cao, X., Ito, Y., 2003. Supercritical fluid extraction of grape seed oil and subsequent separation of free fatty acids by high-speed counter-current chromatography. *J. Chromatogr. A* 1021, 117–124. <https://doi.org/10.1016/j.chroma.2003.09.001>.
- Capanema, E.A., Balakshin, M., 2015. Plantrose lignins: a new type of technical lignins. 18th Int. Symp. Wood, Fibre Pulping Chem 120–123.
- Capolupo, L., Faraco, V., 2016. Green methods of lignocellulose pretreatment for biorefinery development. *Appl. Microbiol. Biotechnol.* 100, 9451–9467. <https://doi.org/10.1007/s00253-016-7884-y>.
- Cocero, M.J., Cabeza, Á., Abad, N., Adamovic, T., Vaquerizo, L., Martínez, C.M., Pazo-Cepeda, M.V., 2018. Understanding biomass fractionation in subcritical & supercritical water. *J. Supercrit. Fluids* 133, 550–565. <https://doi.org/10.1016/j.supflu.2017.08.012>.
- Daz, F.R., Godoy, A., Moreno, J., Bermejo, J.C., Sánchez, C.O., Opazo, A., Gargallo, L., 2001. Blends of vinyllic copolymer with plasticized lignin: thermal and mechanical properties. *J. Appl. Polym. Sci.* 81, 861–874. <https://doi.org/10.1002/app.1505>.
- Donohoe, B.S., Decker, S.R., Tucker, M.P., Himmel, M.E., Vinzant, T.B., 2008. Visualizing lignin coalescence and migration through maize cell walls following thermochemical pretreatment. *Biotechnol. Bioeng.* 101, 913–925. <https://doi.org/10.1002/bit.21959>.
- Duba, K.S., Casazza, A.A., Mohamed, H. Ben, Perego, P., Fiori, L., 2015. Extraction of polyphenols from grape skins and defatted grape seeds using subcritical water: experiments and modeling. *Food Bioprod. Process.* 94, 29–38. <https://doi.org/10.1016/j.fbp.2015.01.001>.
- Ehara, K., Takada, D., Saka, S., 2005. GC-MS and IR spectroscopic analyses of the lignin-derived products from softwood and hardwood treated in supercritical water. *J. Wood Sci.* 51, 256–261. <https://doi.org/10.1007/s10086-004-0653-z>.
- Fiori, L., Lavelli, V., Duba, K.S., Sri Harsha, P.S.C., Mohamed, H. Ben, Guella, G., 2014. Supercritical CO<sub>2</sub> extraction of oil from seeds of six grape cultivars: modeling of mass transfer kinetics and evaluation of lipid profiles and tocol contents. *J. Supercrit. Fluids* 94, 71–80. <https://doi.org/10.1016/j.supflu.2014.06.021>.
- Hames, R., Scarlata, C., Sluiter, A., 2008. Determination of Protein Content in Biomass - NREL/TP-510-42625. NREL.
- Hatakeyama, H., Tsujimoto, Y., Zarubin, M.J., Krutov, S.M., Hatakeyama, T., 2010. Thermal decomposition and glass transition of industrial hydrolysis lignin. *J. Therm. Anal. Calorim.* 101, 289–295. <https://doi.org/10.1007/s10973-010-0698-8>.
- He, J., Huang, Caoxing, Lai, C., Huang, Chen, Li, X., Yong, Q., 2018. Elucidation of structure-inhibition relationship of monosaccharides derived pseudo-lignin in enzymatic hydrolysis. *Ind. Crop. Prod.* 113, 368–375. <https://doi.org/10.1016/j.indcrop.2018.01.046>.
- He, J., Huang, Caoxing, Lai, C., Huang, Chen, Li, M., Pu, Y., Ragauskas, A.J., Yong, Q., 2020. The effect of lignin degradation products on the generation of pseudo-lignin during dilute acid pretreatment. *Ind. Crop. Prod.* 146, 1–8. <https://doi.org/10.1016/j.indcrop.2020.112205>.
- Hemmilä, V., Hosseinpouria, R., Adamopoulos, S., Eceiza, A., 2020. Characterization of wood-based industrial biorefinery lignosulfonates and supercritical water hydrolysis lignin. *Waste and Biomass Valorization* 11, 5835–5845. <https://doi.org/10.1007/s12649-019-00878-5>.
- Hendriks, A.T.W.M., Zeeman, G., 2009. Pretreatments to enhance the digestibility of lignocellulosic biomass. *Bioresour. Technol.* 100, 10–18. <https://doi.org/10.1016/j.biortech.2008.05.027>.
- Jung, Y.H., Kim, K.H., 2015. Acidic pretreatment. *Pretreat. Biomass Process. Technol.* 27–50. <https://doi.org/10.1016/B978-0-12-800080-9.00003-7>.
- Kristensen, J.B., Thygesen, L.G., Felby, C., Jørgensen, H., Elder, T., 2008. Cell-wall structural changes in wheat straw pretreated for bioethanol production. *Biotechnol. Biofuels* 1, 1–9. <https://doi.org/10.1186/1754-6834-1-5>.
- Lancefield, C.S., Wienk, H.J., Boelens, R., Weckhuysen, B.M., Bruijninx, P.C.A., 2018. Identification of a diagnostic structural motif reveals a new reaction intermediate and condensation pathway in kraft lignin formation. *Chem. Sci.* 9, 6348–6360. <https://doi.org/10.1039/c8sc02000k>.
- Li, M., Pu, Y., Ragauskas, A.J., 2016. Current understanding of the correlation of lignin structure with biomass recalcitrance. *Front. Chem.* 4, 1–8. <https://doi.org/10.3389/fchem.2016.00045>.
- Loow, Y.L., Wu, T.Y., Jahim, J.M., Mohammad, A.W., Teoh, W.H., 2016. Typical conversion of lignocellulosic biomass into reducing sugars using dilute acid hydrolysis and alkaline pretreatment. *Cellulose* 23, 1491–1520. <https://doi.org/10.1007/s10570-016-0936-8>.
- Lorenci Woiciechowski, A., Dalmas Neto, C.J., Porto de Souza Vandenberghe, L., de Carvalho Neto, D.P., Novak Sydney, A.C., Letti, L.A.J., Karp, S.G., Zevallos Torres, L.A., Soccol, C.R., 2020. Lignocellulosic biomass: acid and alkaline pretreatments and their effects on biomass recalcitrance – conventional processing and recent advances. *Bioresour. Technol.* 304, 122848. <https://doi.org/10.1016/j.biortech.2020.122848>.
- Maier, T., Schieber, A., Kammerer, D.R., Carle, R., 2009. Residues of grape (*Vitis vinifera* L.) seed oil production as a valuable source of phenolic antioxidants. *Food Chem.* 112, 551–559. <https://doi.org/10.1016/j.foodchem.2008.06.005>.
- Marqués, J.L., Porta, G., Della Reverchon, E., Renuncio, J.A.R., Mainar, A.M., 2013. Supercritical antisolvent extraction of antioxidants from grape seeds after vinification. *J. Supercrit. Fluids* 82, 238–243. <https://doi.org/10.1016/j.supflu.2013.07.005>.
- Martínez, C.M., Cantero, D.A., Bermejo, M.D., Cocero, M.J., 2015. Hydrolysis of cellulose in supercritical water: reagent concentration as a selectivity factor. *Cellulose* 22, 2231–2243. <https://doi.org/10.1007/s10570-015-0674-3>.
- Martínez, C.M., Cantero, D.A., Cocero, M.J., 2018. Production of saccharides from sugar beet pulp by ultrafast hydrolysis in supercritical water. *J. Clean. Prod.* 204, 888–895. <https://doi.org/10.1016/j.jclepro.2018.09.066>.
- Martínez, C.M., Adamovic, T., Cantero, D.A., Cocero, M.J., 2019. Scaling up the production of sugars from agricultural biomass by ultrafast hydrolysis in supercritical water. *J. Supercrit. Fluids* 143, 242–250. <https://doi.org/10.1016/j.supflu.2018.08.017>.
- Moon, S.J., Eom, I.Y., Kim, J.Y., Kim, T.S., Lee, S.M., Choi, I.G., Choi, J.W., 2011. Characterization of lignin-rich residues remaining after continuous supercritical water hydrolysis of poplar wood (*Populus albaglandulosa*) for conversion to fermentable sugars. *Bioresour. Technol.* 102, 5912–5916. <https://doi.org/10.1016/j.biortech.2011.02.091>.
- Pingali, S.V., Urban, V.S., Heller, W.T., McGaughey, J., O'Neill, H., Foston, M., Myles, D.A., Ragauskas, A., Evans, B.R., 2010. Breakdown of cell wall nanostructure in dilute acid pretreated biomass. *Biomacromolecules* 11, 2329–2335. <https://doi.org/10.1021/bm100455h>.
- Prado, J.M., Lachos-Perez, D., Forster-Carneiro, T., Rostagno, M.A., 2016. Sub- and supercritical water hydrolysis of agricultural and food industry residues for the production of fermentable sugars: a review. *Food Bioprod. Process.* 98, 95–123. <https://doi.org/10.1016/j.fbp.2015.11.004>.
- Prozil, S.O., Evtuguin, D.V., Silva, A.M.S., Lopes, L.P.C., 2014. Structural characterization of lignin from grape stalks (*Vitis vinifera* L.). *J. Agric. Food Chem.* 62, 5420–5428. <https://doi.org/10.1021/jf502267s>.
- Sahoo, S., Seydibeyoglu, M.Ö., Mohanty, A.K., Misra, M., 2011. Characterization of industrial lignins for their utilization in future value added applications. *Biomass Bioenergy* 35, 4230–4237. <https://doi.org/10.1016/j.biombioe.2011.07.009>.
- Selig, M.J., Viamajala, S., Decker, S.R., Tucker, M.P., Himmel, M.E., Vinzant, T.B., 2007. Deposition of lignin droplets produced during dilute acid pretreatment of maize stems retards enzymatic hydrolysis of cellulose. *Biotechnol. Prog.* 23, 1333–1339. <https://doi.org/10.1021/bp0702018>.
- Sluiter, A., Hames, B., Ruiz, R., Scarlata, C., Sluiter, J., Templeton, D., Crocker, D., 2008. Determination of Structural Carbohydrates and Lignin in Biomass - NREL/TP-510-42618. NREL.
- Sluiter, A., Hames, B., Ruiz, R., Scarlata, C., Sluiter, J., Templeton, D., 2008a. Determination of Sugars, Byproducts, and Degradation Products in Liquid Fraction Process Samples - NREL/TP-510-42623. NREL.
- Sluiter, A., Hames, R., Ruiz, R., Scarlata, C., Sluiter, J., Templeton, D., 2008b. Determination of Ash in Biomass - NREL/TP-510-42622. NREL.
- Sluiter, A., Ruiz, R., Scarlata, C., Sluiter, J., Templeton, D., 2008c. Determination of Extractives in Biomass - NREL/TP-510-42619. NREL.
- Solarte-Toro, J.C., Romero-García, J.M., Martínez-Patiño, J.C., Ruiz-Ramos, E., Castro-Galiano, E., Cardona-Alzate, C.A., 2019. Acid pretreatment of lignocellulosic biomass for energy vectors production: a review focused on operational conditions and techno-economic assessment for bioethanol production. *Renew. Sustain. Energy Rev.* 107, 587–601. <https://doi.org/10.1016/j.rser.2019.02.024>.
- Wahyudiono, Sasaki, M., Goto, M., 2008. Recovery of phenolic compounds through the decomposition of lignin in near and supercritical water. *Chem. Eng. Process. Process Intensif.* 47, 1609–1619. <https://doi.org/10.1016/j.cep.2007.09.001>.
- Xiao, L.P., Sun, Z.J., Shi, Z.J., Xu, F., Sun, R.C., 2011. Impact of hot compressed water pretreatment on the structural changes of woody biomass for bioethanol production. *BioResources* 6, 1576–1598. <https://doi.org/10.15376/biores.6.2.1576-1598>.
- Xu, F., Yu, J., Tesso, T., Dowell, F., Wang, D., 2013. Qualitative and quantitative analysis of lignocellulosic biomass using infrared techniques: a mini-review. *Appl. Energy* 104, 801–809. <https://doi.org/10.1016/j.apenergy.2012.12.019>.
- Yang, H., Yan, R., Chen, H., Lee, D.H., Zheng, C., 2007. Characteristics of hemicellulose, cellulose and lignin pyrolysis. *Fuel* 86, 1781–1788. <https://doi.org/10.1016/j.fuel.2006.12.013>.
- Łukajtis, R., Rybarczyk, P., Kucharska, K., Konopacka-Lyskawa, D., Stupek, E., Wygodnik, K., Kamiński, M., 2018. Optimization of saccharification conditions of lignocellulosic biomass under alkaline pre-treatment and enzymatic hydrolysis. *Energies* 11. <https://doi.org/10.3390/en11040886>.